

# Synthesize of a novel $^{89}\text{Zr}$ labeled HER2 affibody and its application study in tumor PET imaging

**Yuping Xu**

Jiangsu Institute of Nuclear Medicine

**Lizhen Wang**

Jiangsu Institute of Nuclear Medicine

**Donghui Pan**

Jiangsu Institute of Nuclear Medicine

**Junjie Yan**

Jiangsu Institute of Nuclear Medicine

**Xinyu Wang**

Jiangsu Institute of Nuclear Medicine

**Runlin Yang**

Jiangsu Institute of Nuclear Medicine

**Mingzhu Li**

Inner Mongolia Medical University

**Yu Liu**

Nanjing Medical University

**Min Yang** (✉ [yangmin@jsinm.org](mailto:yangmin@jsinm.org))

---

## Original research

**Keywords:** Human epidermal growth factor receptor-2, PET, affibody,  $^{89}\text{Zr}$

**Posted Date:** March 20th, 2020

**DOI:** <https://doi.org/10.21203/rs.3.rs-18136/v1>

**License:**   This work is licensed under a Creative Commons Attribution 4.0 International License.

[Read Full License](#)

---

**Version of Record:** A version of this preprint was published at EJNMMI Research on June 3rd, 2020. See the published version at <https://doi.org/10.1186/s13550-020-00649-7>.

# Abstract

**Background:** Human epidermal growth factor receptor-2 (HER2) is an important biomarker for tumor diagnosis and therapy. Affibody is an ideal vector for preparing HER2 specific probes due to the advantages such as high affinity and rapid blood clearance etc.  $^{89}\text{Zr}$  is a novel PET imaging isotope with long half-lives and suitable for tracking biological processes for longer periods. In this study, a novel  $^{89}\text{Zr}$  labeled HER2 affibody,  $^{89}\text{Zr}$ -DFO-MAL-Cys-MZHER2, was synthesized and its imaging properties were also evaluated. **Results:** The precursors, DFO-MAL-Cys-MZHER2, were obtained with the yields of nearly 50%. The yields of  $^{89}\text{Zr}$ -DFO-MAL-Cys-MZHER2 were  $90.2 \pm 1.9\%$  and the radiopurities were more than 95%. The total synthesis time was only 30 minutes. The probes were stable in PBS and serum. The tracer accumulated in HER2 overexpression human ovarian cancer SKOV-3 cells. In vivo studies in mice bearing tumors showed that the probe highly retained in SKOV-3 xenografts even for 48 hours. The tumors were visualized with good contrast to normal tissue. ROI analysis revealed that the average uptakes in the tumor were greater than 5 %ID/g. On the contrary, the counterparts of MCF-7 tumors kept low levels of  $\sim 1\% \text{ID/g}$ . The outcome was consistent with the immunohistochemical analysis and ex vivo autoradiography. The probe quickly cleared from the blood and normal organs, and mainly excreted through the urinary system. **Conclusion:** The novel HER2 affibody for PET imaging was easily prepared with satisfactory labeling yield and radiochemical purity.  $^{89}\text{Zr}$ -DFO-MAL-MZHER is a potential candidate for monitoring HER2 expression and may play specific roles in clinical cancer theranostics.

## Introduction

Targeting of hallmarks in cancers with specific agents is a promising strategy in the management of malignancies.<sup>[1]</sup> Human epidermal growth factor receptor type 2 (HER2) is a 185-kDa transmembrane protein and belongs to the family of receptor tyrosine kinases. It involved in the signal transduction pathways regulating cell motility and proliferation. Overexpression of HER2 was found in various solid tumors including ovarian, breast, lung, gastric, colon cancers, etc and associated with aggressiveness, recurrence, and poor survival.<sup>[2–4]</sup> Thus, HER2 is an important clinical tumor biomarker and therapeutic target.

Monoclonal antibodies such as trastuzumab and pertuzumab etc have been approved for the treatment of HER2-positive cancers and the efficacy is satisfactory.<sup>[5–7]</sup> The current selection of patients for HER2 targeted therapy is mainly dependent on the HER2 status determined by biopsy using immunohistochemistry or fluorescence in situ hybridization.<sup>[8]</sup> However, the invasive method may not be reliable due to the heterogeneous expression of the receptor and its dynamic changes during the progress of the disease.<sup>[9]</sup> Almost 20% of the results from the method was reported to be inaccurate.<sup>[10]</sup>

Noninvasive molecular imaging techniques such as Single Photon Emission Computed Tomography (SPECT) and Positron Emission Tomography (PET) provides a reliable method for repetitive investigating the distribution of the receptor in the whole body.<sup>[11, 12]</sup> Compared with SPECT, PET has higher image resolution and quality. PET scanner can sensitively detect gamma radiation from positron decay of

nuclides (e.g.,  $^{11}\text{C}$ ,  $^{18}\text{F}$ ). Due to its high sensitivity, PET imaging with a trace quantity of radiotracers ( $10^{-6}$ – $10^{-8}$  grams) can accurately measure molecular targets in the living body without perturbing the biological system. PET with specific probes is a benefit for disease diagnosis and monitoring therapeutic response.<sup>[13–15]</sup> Radiolabeled antibodies have shown promise in identifying the presence of HER2 in the tumor.<sup>[16–18]</sup> For example,  $^{89}\text{Zr}$ -trastuzumab PET/CT detected unsuspected HER2-positive metastases in patients with HER2-negative primary breast cancer.<sup>[19]</sup> It also found lesions in patients with metastatic HER2-positive esophagogastric cancer<sup>[20]</sup>. However, the optimal images with favorable contrasts should be acquired several days (3–5 days) after administration of the antibodies because of large molecular size (150 kDa), slow tumor penetration and long half-life in circulation.<sup>[19]</sup>

Affibody, an engineered small protein (~7 kDa) that originated from the IgG-binding staphylococcal protein A, is an alternative ligand towards HER2. It is an ideal compound for recognizing the desired targets due to ease of chemical synthesis, quick tumor accumulation and rapid blood clearance, etc.<sup>[21, 22]</sup> ZHER<sub>2:342</sub> affibody specifically binds to HER2 and its derivatives have been labeled with PET nuclides ( $^{18}\text{F}$ ,  $^{68}\text{Ga}$ , etc).<sup>[23–25]</sup>  $^{18}\text{F}$  labeled ZHER<sub>2:342</sub> analog,  $^{18}\text{F}$ -FBEM-ZHER<sub>2:342</sub> showed specific binding towards HER2-positive tumors and might be benefit for monitoring status of the receptor in response to therapeutic interventions.<sup>[23, 26]</sup>  $^{68}\text{Ga}$  labeled HER2 affibody,  $^{68}\text{Ga}$ -ABY-025, discriminated HER2 positive and negative metastatic breast tumor in sixteen patients. After PET/CT scan with the tracer, targeted treatment was changed in three patients<sup>[27, 28]</sup>.

Besides the above short half-life radionuclide, few HER2 affibodies labeled with other PET radioisotopes is rarely reported.  $^{89}\text{Zr}$  is an attractive commercial available PET radionuclide for the long half-life ( $T_{1/2}$  = 78.4 hours), which allows for imaging of biological processes at late time points.<sup>[29]</sup> Meanwhile, attachment of  $^{89}\text{Zr}$  to deferoxamine (DFO) chelator coupled in bioactive substance (such as protein, peptides, etc) can be achieved under mild conditions with good stability.<sup>[30]</sup> Besides,  $^{89}\text{Zr}$ -labeled substances is also an ideal surrogate for the corresponding therapeutic  $^{90}\text{Y}$ -or  $^{177}\text{Lu}$ -labeled radiopharmaceuticals to calculate dosimetry and plan therapy program in preclinical as well as clinical studies.<sup>[31]</sup>

Previous studies have shown that  $^{18}\text{F}$  or  $^{68}\text{Ga}$  labeled modified HER2 affibody with a novel hydrophilic linker,  $^{18}\text{F}$ AI/ $^{68}\text{Ga}$ -NOTA-Cys-GGGRDN-ZHER<sub>2:342</sub> (denoted as  $^{18}\text{F}$ AI/ $^{68}\text{Ga}$ -NOTA-Cys-MZHER2), owned satisfactory specific tumor uptakes and favorable tumor to muscle and blood ratios during 4 hours after injection.<sup>[32, 33]</sup> Due to short half-life, further evaluating the properties of the affibody was difficult beyond 12 hours. To better evaluate the characters of the modified HER2 affibody, the molecule was coupled with a maleimide derivative of desferrioxamine, MAL-DFO, then radiolabeled with  $^{89}\text{Zr}$ . The efficiency of the resulting probe,  $^{89}\text{Zr}$ -DFO-MAL-Cys-MZHER2 targeting HER2 was also investigated in tumor models.

## Methods

Cys-ZHER<sub>2:342</sub> and Cys-MZHER2 were purchased from Apeptide Co., Ltd. (Shanghai, China). MAL-DFO was purchased from Macrocyclics (Dallas, TX). [<sup>89</sup>Zr]-oxalate solution was supplied by Cyclotron VU (Netherlands). Human ovarian cancer cell lines SKOV-3 and breast cancer cell lines MCF-7 were purchased from Cell Bank of Shanghai Institutes for Biological Sciences. Female Balb/c nude mice were purchased from SLAC Laboratory Animal Co., Ltd., China. Analytic and preparative high-performance liquid chromatography (HPLC) was performed according to the previous literatures.<sup>[32, 33]</sup> Radio thin-layer chromatography (TLC) was operated on silica gel impregnated glass fiber sheets and analyzed by a BioScan. Sodium citrate solutions (0.1M) was used as solvent systems. Mass spectra were obtained with a Waters LC-MS system (Waters, Milford, MA) that included an Acquity UPLC system coupled to a Waters Q-ToF Premier high-resolution mass spectrometer

## Affibody Conjugation

MAL-DFO (0.35mg, 0.50μmol) was dissolved in ammonium acetate solution and reacted with Cys-MZHER2 (3mg, 0.40μmol) at room temperature overnight. (Figure 1) The product was purified with preparative HPLC followed by lyophilization as previously described.<sup>[32]</sup> Mass spectrometry (MS) measured m/z 8077.5 for [MH]<sup>+</sup> (C<sub>351</sub>H<sub>560</sub>N<sub>104</sub>O<sub>111</sub>S<sub>2</sub>„ calculated molecular weight 8076.8).

## Preparing of <sup>89</sup>Zr-DFO-MAL-Cys-MZHER2

DFO conjugated affibody, DFO-MAL-Cys-MZHER2,(200μg,25nmol) was dissolved in 30μL deionized water and incubated with 185MBq [<sup>89</sup>Zr]-oxalate in 2M Na<sub>2</sub>CO<sub>3</sub> solutions (pH = 4) for 20 minutes at room temperature. (Figure 2) After diluted with 10mL deionized water, the complex was purified by a Varian BOND ELUT C18 column. After washing with 10 mL deionized water again, the product was eluted with 0.3mL 10 mM HCl in ethanol. The solution was diluted with 10 mL saline and passed through a 0.22-μm Millipore filter into a sterile vial. Radio HPLC and TLC were used for quality control.

## In vitro stability

Aliquots of <sup>89</sup>Zr-DFO-MAL-Cys-MZHER2 solutions were incubated with human serum or PBS for 48 hours at 37°C. At the preselected time points, the radiopurity was analyzed by TLC.

## Cell lines

Cells were cultured in RPMI-1640 medium supplemented with 10% (v/v) heat-inactivated fetal bovine serum (GIBCO) and grown as a monolayer at 37°C in a humidified atmosphere containing 5% CO<sub>2</sub>.

# Cell uptake studies

Uptake studies of  $^{89}\text{Zr}$ -DFO-MAL-Cys-MZHER2 in SKOV-3 cells were performed according to the method described.<sup>[32]</sup> Cells ( $1 \times 10^6$  / well) were incubated at 37 °C for various times with 37KBq labeled affibodyin a 0.5 mL serum-free DMEM medium. The nonspecific binding of the tracer was determined by co-incubation with 5  $\mu\text{M}$  Cys-ZHER<sub>2:342</sub>. After washed with chilled PBS, the cell pellets in the tube were obtained by centrifugation and measured using a  $\gamma$ -counter (PerkinElmer). The cell uptake was expressed as the percentage of the added dose (%AD/ $10^6$ cells) after decay correction.

## Animal Model

All animal experiments complied with the institutional guidelines and were approved by local authorities. Tumor models were established by subcutaneously implanted  $5 \times 10^6$  SKOV-3 or MCF-7 tumor cells suspended in 0.2 mL PBS into the shoulder region of mice. When tumor sizes reached 100–300 mm<sup>3</sup>, the mice were used for the following experiments.

## MicroPET Imaging

PET imaging was performed on a microPET scanner (Siemens Inc.). Under isoflurane anesthesia, the mice bearing tumors were placed prone in the center of the scanner and injected into 3.7 MBq  $^{89}\text{Zr}$ -DFO-MAL-Cys-MZHER2 with or without excessive non-labeled Cys-MZHER<sub>2:342</sub> (10mg/kg body weight) via the lateral tail vein. Static PET images of 10 minutes were performed at selected times after tracer injection. Quantitative analysis of PET images was performed using the same method as previously reported.<sup>[32, 33]</sup>

## Biodistribution

Mice were injected with 0.74 MBq of the tracer via the tail vein and sacrificed at 1, 4, 8, 18, 24, 48 and 72 hour after administration respectively. For a blocking study, four mice were coinjected with an excess of unlabeled Cys-ZHER<sub>2:342</sub> (10mg/kg body weight) and killed at 1 hour after administration. Tumor and normal tissues of interest were removed and weighed. The radioactivity uptake in the organs was measured in the  $\gamma$ -counter and expressed as a percentage of the injected radioactive dose per gram of tissue (% ID/g).

## Autoradiography and Histology

After microPET imaging, the tumors were harvested and sectioned into slices with 5µm thickness at – 80°C. Ex vivo autoradiography was conducted using the previous method<sup>[34]</sup>. To determine the intratumoral distribution of the tracer, the slices were placed on a phosphorimaging plate for 1 hour. Phosphorimaging plates were read with a plate reader. Quantitative analysis was carried out using OptiQuant software.

Allowing radioactive decay, the slices were used for routine HE staining and HER2 analysis by immunohistochemistry. The procedures were processed following the published literature<sup>[33]</sup>. An epifluorescence microscope (Olympus, X81, Japan) was used to acquire the corresponding images.

## Statistical Analysis

Statistical analyses were performed using GraphPad Prism. Data were analyzed using the unpaired, 2-tailed Student t-test. Differences at the 95% confidence level ( $p < 0.05$ ) were considered to be statistically significant.

## Results

### Chemistry

DFO conjugated affibody was readily prepared with a yield of 50%. The chemical purity of the compound was greater than 90% determined by analytical HPLC.

### Radiolabeling Chemistry

The non-decay corrected yield for  $^{89}\text{Zr}$ -DFO-MAL-Cys-MZHER2 was  $90.2 \pm 1.2\%$  respectively. Purification using C18 columns provided a radiochemical purity of more than 95%. HPLC analysis of the tracer showed one single peak with a retention time of 14 minutes (Figure 3).  $^{89}\text{Zr}$ -DFO-MAL-Cys-MZHER2 showed a typical elution profile ( $R_f = 0.2-0.3$ ) on radio TLC. In comparison, free [ $^{89}\text{Zr}$ ]-oxalate run into the solvent front ( $R_f = 0.8-1.0$ )

### Stability Studies In Vitro

$^{89}\text{Zr}$ -DFO-MAL-Cys-MZHER2 was stable for the investigated periods. No free [ $^{89}\text{Zr}$ ]-oxalate was found after incubation of the tracer in PBS or serum for 2 days at 37°C.

### Cell Uptake

Cell uptake studies are shown in Figure 5. The probe quickly accumulated in SKOV-3 and reached plateaus with  $10.23 \pm 0.94$  %AD/ $10^6$  cells at 30 minutes incubation. By contrast, the uptake levels were significantly decreased in the presence of excess unlabeled Cys-ZHER<sub>2:342</sub> at the same time points ( $2.35 \pm 0.43$  %AD/ $10^6$  cells).

## Small-Animal PET Imaging

Decay-corrected coronal microPET images of mice bearing tumors were shown in Figure 6 and Figure 7. SKOV-3 xenografts were clearly visualized with good contrast even after 48 hours of administration. The SKOV-3 tumor uptakes of the tracer were  $11.97 \pm 2.52$ ,  $11.43 \pm 2.51$ ,  $10.09 \pm 2.83$ ,  $8.52 \pm 1.15$ ,  $7.51 \pm 0.39$  and  $4.99 \pm 1.68$  %ID/g at 1, 4, 8, 10, 24 and 48 hours after administration respectively. In contrast, the radio signals in MCF-7 xenografts were weak. The MCF-7 tumor uptakes were  $1.98 \pm 0.28$ ,  $1.79 \pm 0.29$ ,  $1.39 \pm 0.14$  and  $1.21 \pm 0.10$  %ID/g at 1, 4, 8 and 24 hours after administration respectively. Presaturation of HER2 in tumors by co-injection of nonlabeled Cys-MZHER<sub>2:342</sub> caused a significant reduction of radioactivity accumulation in tumors ( $2.18 \pm 0.23$  %ID/g at 60 minutes postinjection).

It also showed that the liver uptake was very low, with the highest being about 2 %ID/g at 60 min after injection. Prominent uptake was also observed in kidneys, which suggested that the tracer is mainly excreted through the renal-urinary route.

## Biodistribution Studies

The biodistribution data of <sup>89</sup>Zr-labeled affibody in mice bearing tumors are presented in Tables 1. Consistent with PET imaging, radioactivity concentration in SKOV-3 tumors was higher than those in MCF-7 tumors and other healthy organs except for kidneys. Accumulation in SKOV-3 tumors was  $11.27 \pm 1.55$  %ID/g at 1 hour after administration and maintained  $8.20 \pm 0.82$  %ID/g at 24 hours postinjection. <sup>89</sup>Zr-DFO-MAL-Cys-MZHER2 uptake in the MCF-7 tumors was  $1.76 \pm 0.31$  %ID/g at 1 hour postinjection. Under block with unlabeled HER2 affibody, the SKOV-3 tumor uptake of the tracer significantly reduced to  $1.87 \pm 0.15$  %ID/g at the same time point.

A rapid washout of radioactivity was noted from receptor-negative tissues except kidney. The uptake ratios of tumor-to-blood and tumor to muscle values increased from  $8.38 \pm 3.73$  and  $17.80 \pm 3.08$  at 1 hour postinjection to  $89.00 \pm 12.89$  and  $138.07 \pm 18.63$  at 24 hours postinjection in mice bearing SKOV-3 tumors respectively.

## Ex vivo Autoradiography and Histology

Autoradiography studies showed that higher radioactivity accumulated in the periphery of tumors than those at internal tissues. The ratios of radioactive intensity between the two regions were determined to

be  $5.03 \pm 0.69$ .

The pathological analysis confirmed that the peripheral of tumor tissue grew vigorously, and the HER2 receptor was overexpressed. On the contrary, the internal tumor tissue grew slowly even died with low levels of HER2. The results were consistent with the findings by autoradiography.

## Discussion

Molecular imaging offers a non-invasive method for measuring receptor levels of the entire disease burden. The use of PET might enhance the accuracy of characterizing tumor biology and help in identifying therapeutic targets and making personalized treatment. Radiopharmaceuticals play a critical role in PET imaging. Although  $^{18}\text{F}$  and  $^{68}\text{Ga}$  are conventional isotopes for clinical application, short half-life limited their use in studying the pharmacokinetics of biomolecules at later time points.

$^{89}\text{Zr}$  is an emerging PET nuclide for long-circulating targeting vectors due to its long half-life. Meanwhile,  $^{89}\text{Zr}$  exhibits high resolution PET images because of its relatively low translational energy (389KeV), which is between  $^{18}\text{F}$  (250 keV) and  $^{68}\text{Ga}$  (836 keV). Interestingly,  $^{89}\text{Zr}$  also can be used for in vivo Cerenkov luminescence imaging and could be benefit for image-guided surgery.<sup>[31]</sup> Thus,  $^{89}\text{Zr}$  has shown great potential in PET imaging during the last decades.

Affibody ZHER<sub>2:342</sub> is a specific ligand targeting HER2. Previous short-lived positron-emitting nuclides ( $^{18}\text{F}$ ,  $^{68}\text{Ga}$ ) labeled ZHER<sub>2:342</sub> derivatives could only be used as imaging for a few hours (at most 6 hours).<sup>[28, 32, 33]</sup>  $^{89}\text{Zr}$  labeled affibody might provide more information about the pharmacokinetics of the tracer, which is in favor of the development of radiolabeled bioactive compounds with therapeutic isotope. Herein,  $^{89}\text{Zr}$  labeled HER2 affibody,  $^{89}\text{Zr}$ -DFO-MAL-MZHER2, was designed and synthesized. The specificity and imaging properties of the tracer were also evaluated in tumor models.

Desferrioxamine is a hexadentate chelator used for treatment the iron overload. It is consisted of three hydroxamate groups and forms a thermodynamically stable complex with zirconium.<sup>[35]</sup> For site-specific labeling, deferoxamine-maleimide (MAL-DFO) was successfully introduced into MZHER2 by conjugated the thiol group in cysteine residue with the maleimide.  $^{89}\text{Zr}$  attached to DFO-MAL-Cys-MZHER2 under mild conditions with nearly quantitative yields. The radiochemical purity was satisfactory determined by both HPLC and TLC. Absence of radiolysis was detected in PBS and serum during in vitro incubation up 48 hours. The stability was derived from an octadentate complex structure and familiar with the other  $^{89}\text{Zr}$ -DFO compounds. It means that  $^{89}\text{Zr}$  radiolabeled affibody could be prepared at least one day before preclinical or clinical PET studies.

Similar to  $^{18}\text{F}$  or  $^{68}\text{Ga}$  labeled affibody, the  $^{89}\text{Zr}$  labeled counterpart specifically binds to HER2-positive SKOV-3 tumor cells by in vitro cell uptake experiments. It meant that coupling the affibody with DFO-MAL could not significantly affect the performance of binding to the receptor.



To better understand the biology characters of the affibody, in vivo experiments including biodistribution studies and microPET imaging were firstly conducted in SKOV-3 and MCF-7 tumor models, which have been often applied for preclinical evaluation the specificity of radiolabeled HER2 affibody. It revealed that  $^{89}\text{Zr}$ -DFO-MAL-Cys-MZHER2 rapidly concerted in SKOV-3 tumors after 1 hour postinjection. The uptake in SKOV-3 tumors was nearly 10 folds higher than those of MCF-7 tumors at any time point. Compared with the blood pool and most of normal organs, the retention of the probe remained stable in SKOV-3 tumors over time. Even after 48 hours post injection, still 40% of the initially accumulated radioactivity was observed in the SKOV-3 xenografts and the image contrast was favorable.

The radioactivities distributing in the tumor showed significant heterogeneity by ex vivo immunohistochemistry and autoradiography. Abundant HER2 was expressed in the periphery of the tumor and the corresponding radio signal was strong. On the contrary, weak radioactivity was detected in the internal necrotic tissues. Receptor specificity was also confirmed by decreasing the tumor uptake with an excess of unlabeled HER2 affibody. It implied that the targeting propriety of  $^{89}\text{Zr}$ -DFO-MAL-Cys-MZHER2 was consistent with the performances of  $^{18}\text{F}$  or  $^{68}\text{Ga}$  labeled MZHER2 affibody.<sup>[32, 33]</sup>

The uptake values in the liver are comparable to those of  $^{18}\text{F}$  or  $^{68}\text{Ga}$  labeled affibody ( $\sim 2\% \text{ID/g}$  at 1 hour p.i. then decrease to  $\sim 1\% \text{ID/g}$  at 4 hour p.i.), which suggested that the modification with a hydrophilic linker was effective to decline abdomen background. Higher kidney uptake was found after blocking since non-bound  $^{89}\text{Zr}$ -DFO-MAL-Cys-MZHER2 was cleared from the blood and re-absorbed in the normal organ. It seemed that the renal uptake of the  $^{89}\text{Zr}$  labeled affibody was not mediated by HER2. It seemed that the re-absorptions of  $^{89}\text{Zr}$ -DFO-MAL-Cys-MZHER2 in the kidney may be mediated by the scavenger receptor systems, which is responsible for recycling proteins from the urines.<sup>[36]</sup> Despite this, high renal uptakes may not prevent the visualization of the tumor near the organ. For example, metastases in the adrenal gland were clearly visualized after administration of  $^{111}\text{In}$ -labeled HER2 affibody,  $^{111}\text{In}$ -ABY-025<sup>[37]</sup>. Low uptakes ( $< 2\% \text{ID/g}$ ) was observed in the bone. It suggested that the in vivo stability of  $^{89}\text{Zr}$ -DFO-MAL-Cys-MZHER2 was good since free  $^{89}\text{Zr}$  accumulates irreversibly in the mineralized bone.

## Conclusion

A novel PET tracer targeting HER2,  $^{89}\text{Zr}$ -DFO-MAL-Cys-MZHER2, was successfully prepared by radiolabeling modified affibody with  $^{89}\text{Zr}$ . Preclinical study revealed that  $^{89}\text{Zr}$ -DFO-MAL-Cys-MZHER2 is a candidate radiotracer for specific, noninvasive detection of HER2 levels in tumors.

## Declarations

## Availability of data and materials

The data generated during the current study are available from the corresponding author on reasonable request.

# Acknowledgements

The authors would like to thank all the participating staff members of Jiangsu Institute of Nuclear Medicine for the study.

## Funding

This work was partially supported by National Natural Science Foundation (81472749,5147307,31671035), National Significant New Drugs Creation Program(2017ZX09304021),Jiangsu Provincial Medical Innovation Team (CXTDA2017024), Jiangsu Provincial Natural Science Foundation (BK20161137–BK20170204–BE2016632),Jiangsu Health International Exchange Program(JSH–2018–015), Jiangsu talent projects (LGY2017088),Jiangsu Provincial Commission of Health and Family Planning Foundation–H2017031, QNRC2016628–,Wuxi Commission of Health and Family Planning Foundation (Q201729).

## Author information

Lizhen Wang contributed equally to this work and share first authorship.

## Contributions

The study design was set up by Yuping Xu, Lizhen Wang, Donghui Pan and Min Yang. Data collection and interpretation was carried out by Lizhen Wang, Xinyu Wang and Yu Liu. Yuping Xu, Junjie Yan and Donghui Pan were responsible for the production of the tracer. The corresponding in vitro and in vivo experiments were performed by Xinyu Wang, Runlin Yang, Mingzhu Li and Yu Liu. Dr Min Yang was the principal investigator of this study. All authors read and approved the final manuscript.

## Corresponding author

Correspondence to Min Yang ([yangmin@jsinm.org](mailto:yangmin@jsinm.org)).

## Ethics approval

All animal experiments complied with the institutional guidelines and were approved by the Ethics Committee of Jiangsu Institute of Nuclear Medicine.

# Consent for publication

Not applicable

## Competing interests

The authors declare that they have no conflict of interest.

## Reference

1. Hanahan D, Weinberg RA. Hallmarks of cancer: the next generation. *Cell*. 2011;144:646–74.
2. Oh D-Y, Bang Y-J. HER2-targeted therapies—a role beyond breast cancer. *Nat Rev Clin Oncol*. 2019;1–16.
3. Pegram MD, Miles D, Tsui CK, Zong Y. HER2-Overexpressing/Amplified Breast Cancer as a Testing Ground for Antibody–Drug Conjugate Drug Development in Solid Tumors. *Clin Cancer Res*. 2019.
4. Domínguez-Ríos R, Sánchez-Ramírez DR, Ruiz-Saray K, Ocegüera-Basurto PE, Almada M, Juárez J, et al. Cisplatin-loaded PLGA nanoparticles for HER2 targeted ovarian cancer therapy. *Colloid Surf B-Biointerfaces*. 2019;178:199–207.
5. Mazzotta M, Krasniqi E, Barchiesi G, Pizzuti L, Tomao F, Barba M, et al. Long-term safety and real-world effectiveness of trastuzumab in breast cancer. *J Clin Med*. 2019;8:254.
6. Bonelli P, Borrelli A, Tuccillo FM, Silvestro L, Palaia R, Buonaguro FM. Precision medicine in gastric cancer. *World J Gastroenterol*. 2019;11:804–29.
7. Eiger D, Pondé NF, de Azambuja E. Pertuzumab in HER2-positive early breast cancer: current use and perspectives. *Future Oncol*. 2019;15:1823–43.
8. Chen Y, Liu L, Ni R, Zhou W. Advances in HER2 testing. *Adv Clin Chem*. 2019;91:123–62.
9. Jauw YW, O'Donoghue JA, Zijlstra JM, Hoekstra OS, Menke-van der Houven CW, Morschhauser F, et al. <sup>89</sup>Zr-Immuno-PET: Toward a Noninvasive Clinical Tool to Measure Target Engagement of Therapeutic Antibodies In Vivo. *J Nucl Med*. 2019;60:1825–32.
10. Massicano AV, Lee S, Crenshaw BK, Aweda TA, El Sayed R, Super I, et al. Imaging of HER2 with [<sup>89</sup>Zr] pertuzumab in Response to T-DM1 Therapy. *Cancer Biother Radiopharm*. 2019;34:209–17.
11. Liang Q, Kong L, Zhu X, Du Y, Tian J. Noninvasive Imaging for Assessment of the Efficacy of Therapeutic Agents for Hepatocellular Carcinoma. *Mol Imaging Biol*. 2019;1–14.

- 12.Mankoff DA, Farwell MD, Clark AS, Pryma DA. Making molecular imaging a clinical tool for precision oncology: a review. *JAMA Oncol.* 2017;3:695–701.
- 13.Menon H, Guo C, Verma V, Simone CB. The Role of Positron Emission Tomography Imaging in Radiotherapy Target Delineation. *PET Clin.* 2020;15:45–53.
- 14.Provost J, Garofalakis A, Sourdon J, Bouda D, Berthon B, Viel T, et al. Simultaneous positron emission tomography and ultrafast ultrasound for hybrid molecular, anatomical and functional imaging. *Nat Biomed Eng.* 2018;2:85–94.
- 15.Marcu LG, Moghaddasi L, Bezak E. Imaging of tumor characteristics and molecular pathways with PET: developments over the last decade toward personalized cancer therapy. *International Journal of Radiation Oncology\* Biology\* Physics.* 2018;102:1165–82.
- 16.Aluicio-Sarduy E, Ellison PA, Barnhart TE, Cai W, Nickles RJ, Engle JW. PET radiometals for antibody labeling. *J Lablled Compd Rad.* 2018;61:636–51.
- 17.Woo S-K, Jang SJ, Seo M-J, Park JH, Kim BS, Kim EJ, et al. Development of <sup>64</sup>Cu-NOTA-Trastuzumab for HER2 Targeting: A Radiopharmaceutical with Improved Pharmacokinetics for Human Studies. *J Nucl Med.* 2019;60:26–33.
- 18.Moek KL, Giesen D, Kok IC, de Groot DJA, Jalving M, Fehrmann RS, et al. Theranostics using antibodies and antibody-related therapeutics. *J Nucl Med.* 2017;58:83S–90S.
- 19.Dehdashti F, Wu N, Bose R, Naughton MJ, Ma CX, Marquez-Nostra BV, et al. Evaluation of [<sup>89</sup>Zr] trastuzumab-PET/CT in differentiating HER2-positive from HER2-negative breast cancer. *Breast Cancer Res Treat.* 2018;169:523–30.
- 20.O'Donoghue JA, Lewis JS, Pandit-Taskar N, Fleming SE, Schöder H, Larson SM, et al. Pharmacokinetics, biodistribution, and radiation dosimetry for <sup>89</sup>Zr-trastuzumab in patients with esophagogastric cancer. *J Nucl Med.* 2018;59:161–6.
- 21.De A, Kuppusamy G, Karri VVSR. Affibody molecules for molecular imaging and targeted drug delivery in the management of breast cancer. *Int J Biol Macromol.* 2018;107:906–19.
- 22.Gebauer M, Skerra A. Engineering of binding functions into proteins. *Curr Opin Biotechnol.* 2019;60:230–41.
- 23.Kramer-Marek G, Bernardo M, Kiesewetter DO, Bagci U, Kuban M, Omer A, et al. PET of HER2-positive pulmonary metastases with <sup>18</sup>F-ZHER2: 342 affibody in a murine model of breast cancer: comparison with <sup>18</sup>F-FDG. *J Nucl Med.* 2012;53:939–46.
- 24.Yanai A, Harada R, Iwata R, Yoshikawa T, Ishikawa Y, Furumoto S, et al. Site-Specific Labeling of F–18 Proteins Using a Supplemented Cell-Free Protein Synthesis System and O–2-[<sup>18</sup>F] Fluoroethyl-L-Tyrosine:

[18 F] FET-HER2 Affibody Molecule. *Mol Imaging Biol.* 2019;21:529–37.

25.Velikyan I, Schweighöfer P, Feldwisch J, Seemann J, Frejd FY, Lindman H, et al. Diagnostic HER2-binding radiopharmaceutical,[68Ga] Ga-ABY-025, for routine clinical use in breast cancer patients. *Am J Nucl Med Mol Imaging.* 2019;9:12–23.

26.Kramer-Marek G, Kiesewetter DO, Martiniova L, Jagoda E, Lee SB, Capala J. [18 F] FBEM-Z HER2: 342-Affibody molecule—a new molecular tracer for in vivo monitoring of HER2 expression by positron emission tomography. *Eur J Nucl Med Mol Imaging.* 2008;35:1008–18.

27.Sandström M, Lindskog K, Velikyan I, Wennborg A, Feldwisch J, Sandberg D, et al. Biodistribution and radiation dosimetry of the anti-HER2 affibody molecule 68Ga-ABY-025 in breast cancer patients. *J Nucl Med.* 2016;57:867–71.

28.Sörensen J, Velikyan I, Sandberg D, Wennborg A, Feldwisch J, Tolmachev V, et al. Measuring HER2-receptor expression in metastatic breast cancer using [68Ga] ABY-025 Affibody PET/CT. *Theranostics.* 2016;6:262–71.

29.Heskamp S, Raavé R, Boerman O, Rijpkema M, Goncalves V, Denat F. 89Zr-immuno-positron emission tomography in oncology: state-of-the-art 89Zr radiochemistry. *Bioconjug Chem.* 2017;28:2211–23.

30.Brandt M, Cardinale J, Aulsebrook ML, Gasser G, Mindt TL. An overview of PET radiochemistry, part 2: Radiometals. *J Nucl Med.* 2018;59:1500–6.

31.Dilworth JR, Pascu SI. The chemistry of PET imaging with zirconium-89. *Chem Soc Rev.* 2018;47:2554–71.

32.Xu Y, Bai Z, Huang Q, Pan Y, Pan D, Wang L, et al. PET of HER2 expression with a novel 18FAl labeled affibody. *J Cancer.* 2017;8:1170–8.

33.Xu Y, Wang L, Pan D, Yu C, Mi B, Huang Q, et al. PET imaging of a 68Ga labeled modified HER2 affibody in breast cancers: from xenografts to patients. *Br J Radiol.* 2019;92:20190425.

34.Mason C, Kossatz S, Carter L, Pirovano G, Brand C, Guru N, et al. A 89Zr-HDL PET tracer monitors response to a CSF1R inhibitor. *J Nucl Med.* 2019;jnumed. 119.230466.

35.Raavé R, Sandker G, Adumeau P, Jacobsen CB, Mangin F, Meyer M, et al. Direct comparison of the in vitro and in vivo stability of DFO, DFO\* and DFOcyclo\* for 89 Zr-immunoPET. *Eur J Nucl Med Mol Imaging.* 2019;46:1966–77.

36.Garousi J, Andersson KG, Mitran B, Pichl M-L, Ståhl S, Orlova A, et al. PET imaging of epidermal growth factor receptor expression in tumours using 89Zr-labelled ZEGFR: 2377 affibody molecules. *Int J Oncol.* 2016;48:1325–32.

37.Sørensen J, Sandberg D, Sandström M, Wennborg A, Feldwisch J, Tolmachev V, et al. First-in-human molecular imaging of HER2 expression in breast cancer metastases using the 111In-ABY-025 affibody molecule. J Nucl Med. 2014;55:730–5.

Table

Due to technical limitations, Table 1 is only available for download from the Supplementary Files section.

Figures

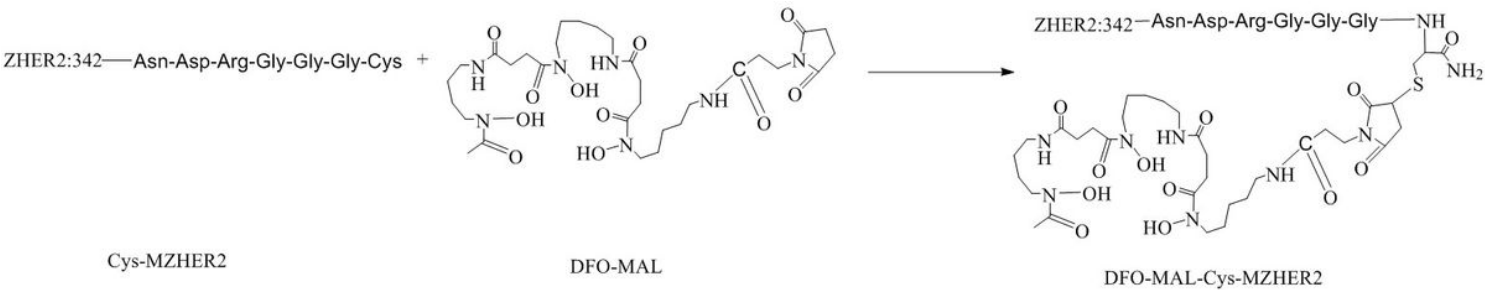


Figure 1

Schemes for synthesis of DFO-MAL-Cys-MZHER2

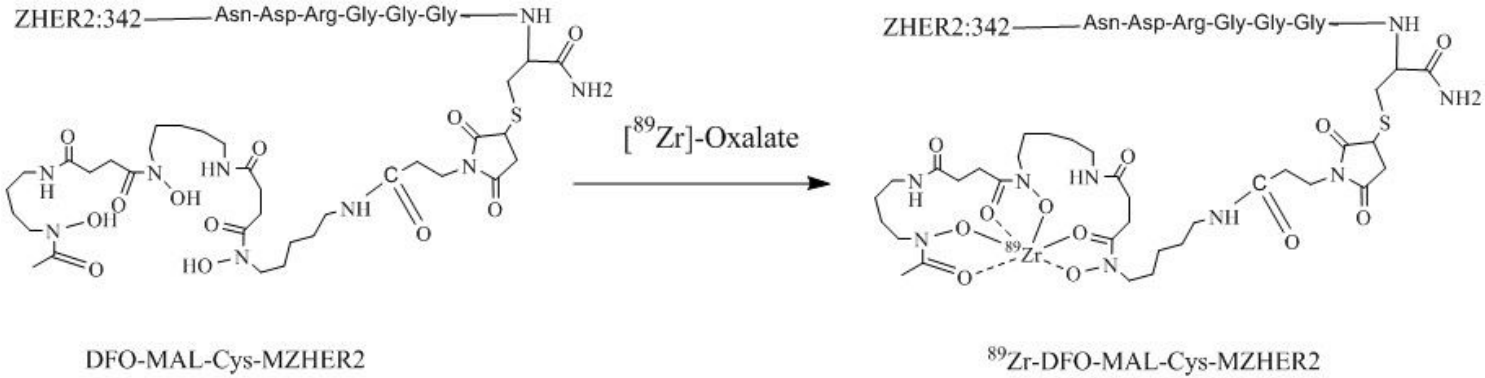
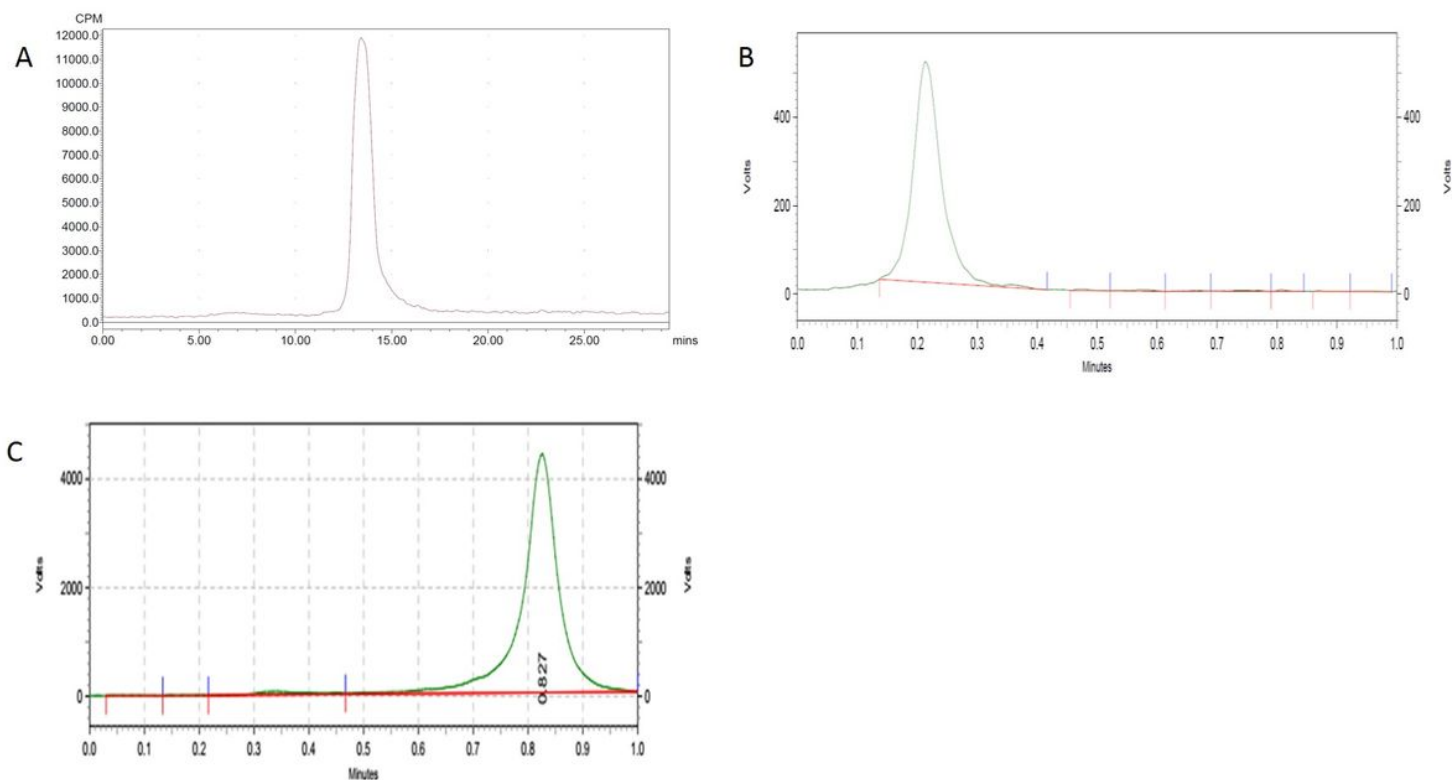


Figure 2

Scheme of radiosynthesis of 89Zr-DFO-MAL-Cys-MZHER2



**Figure 3**

A) HPLC chromatograms of  $^{89}\text{Zr}$ -DFO-MAL-Cys-MZHER2; B) TLC chromatograms of  $^{89}\text{Zr}$ -DFO-MAL-Cys-MZHER2; C) TLC chromatograms of free [ $^{89}\text{Zr}$ ]-oxalate.

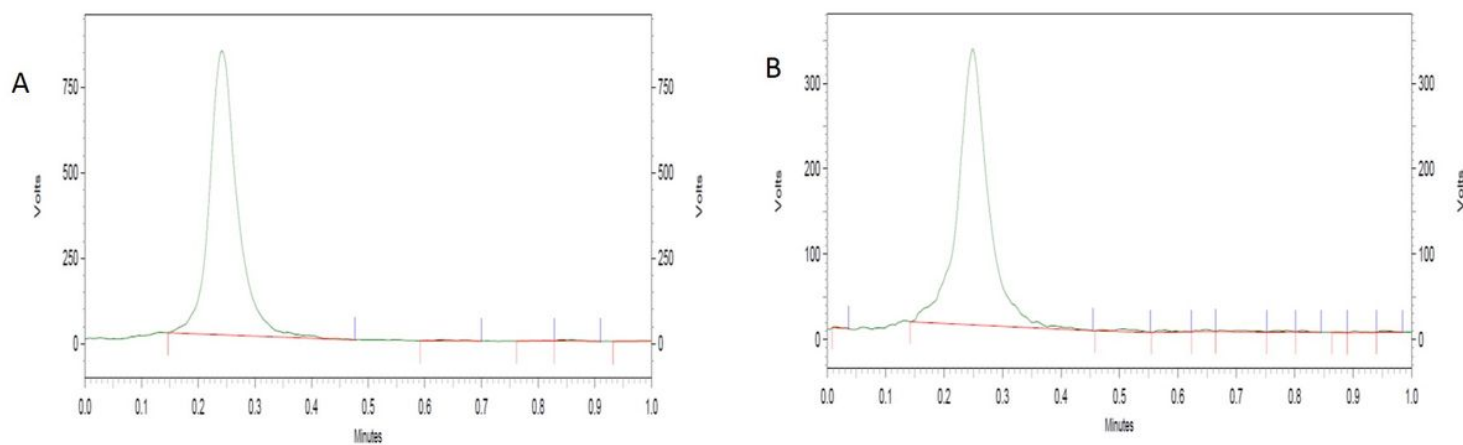


**Figure 4**

TLC chromatograms of  $^{89}\text{Zr}$ -DFO-MAL-Cys-MZHER2 in PBS (A) and serum (B) at  $37^\circ\text{C}$  for 48 hours respectively.

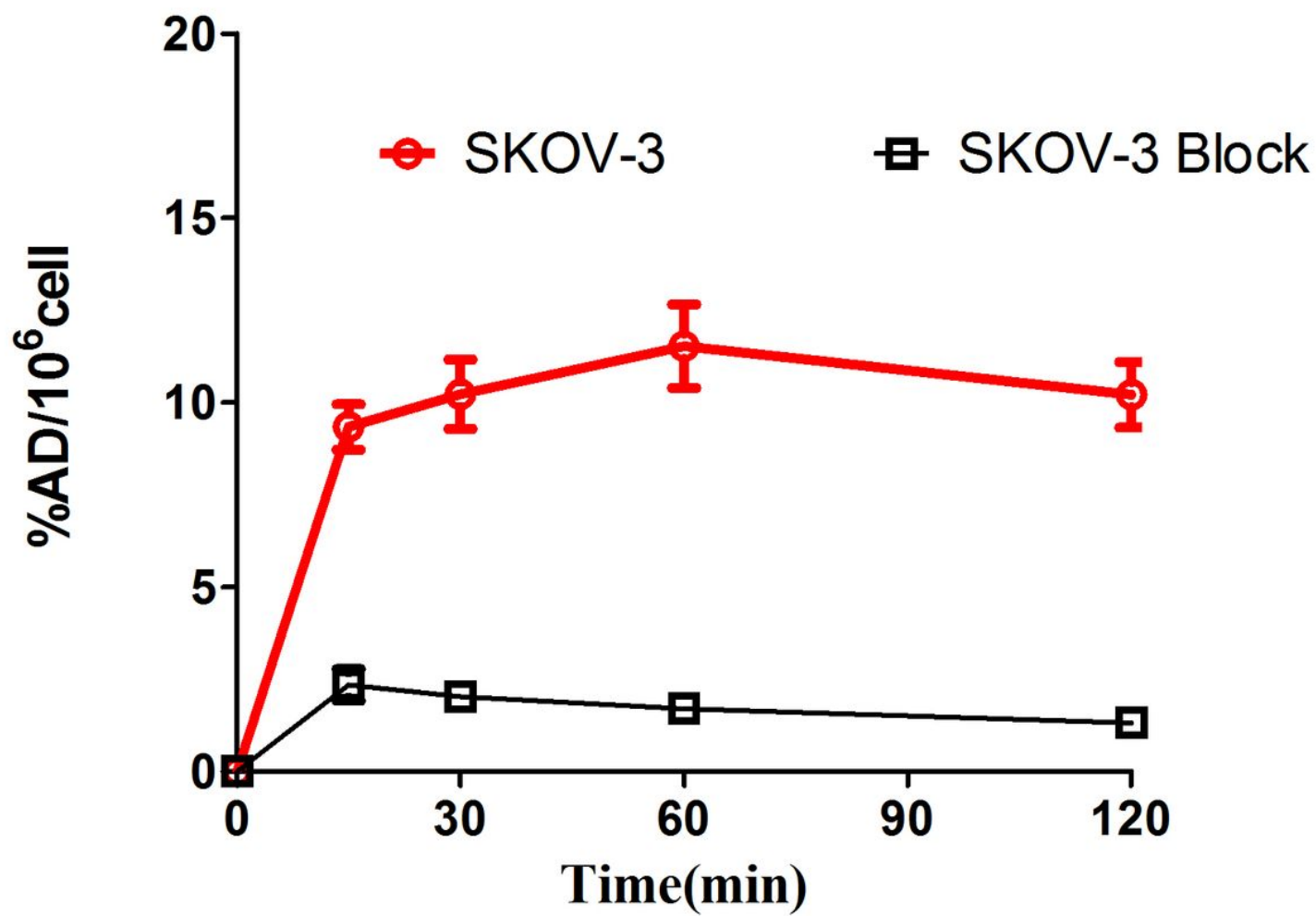
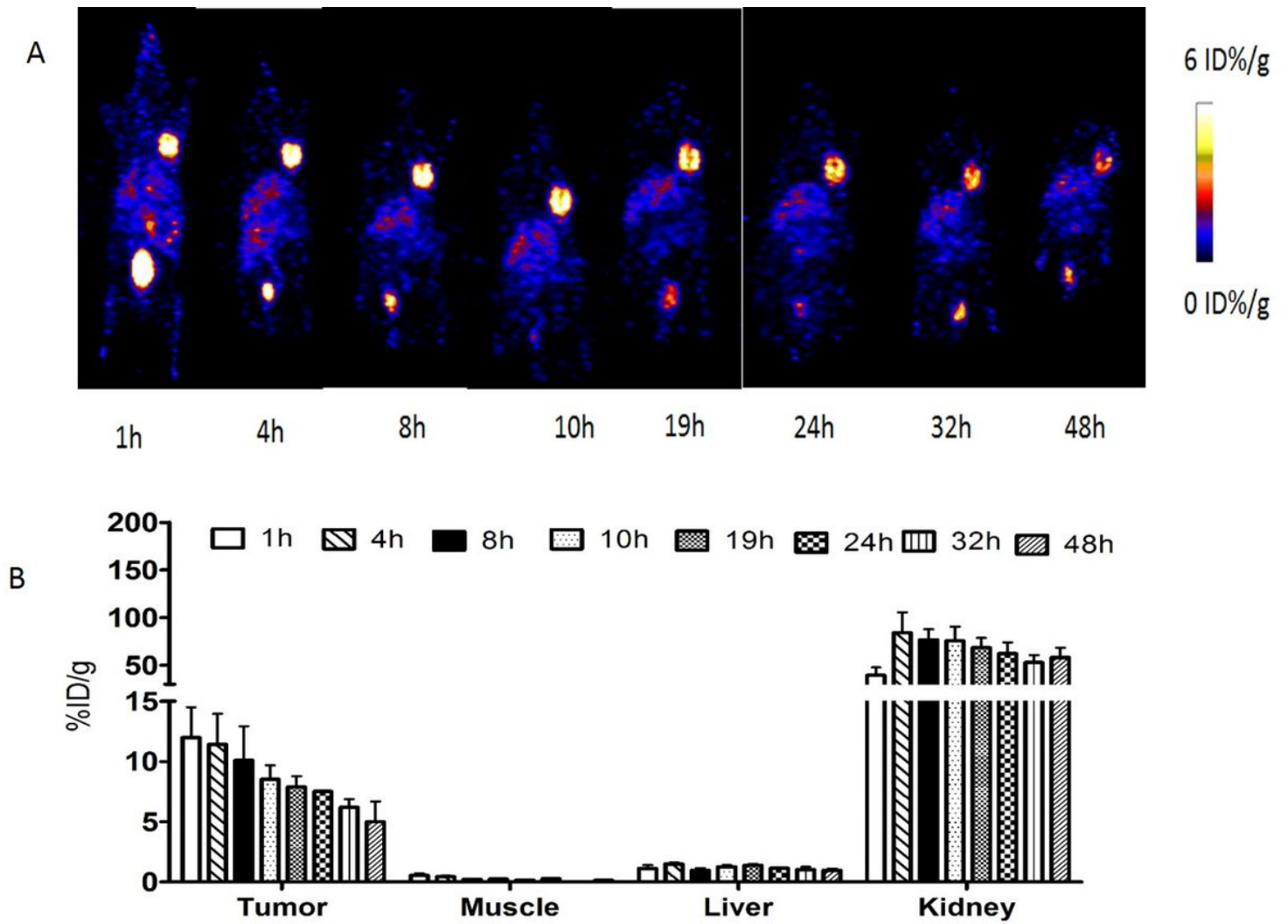


Figure 5

Cell uptake assay of  $^{89}\text{Zr}$ -DFO-MAL-Cys-MZHER2 in SKOV-3 cells.





**Figure 6**

Decay-corrected whole-body PET images of mice bearing SKOV-3 tumors(A) after injection of  $^{89}\text{Zr}$ -DFO-MAL-Cys-MZHER2; B) Quantification of radioactivities in SKOV-3 xenografts models.

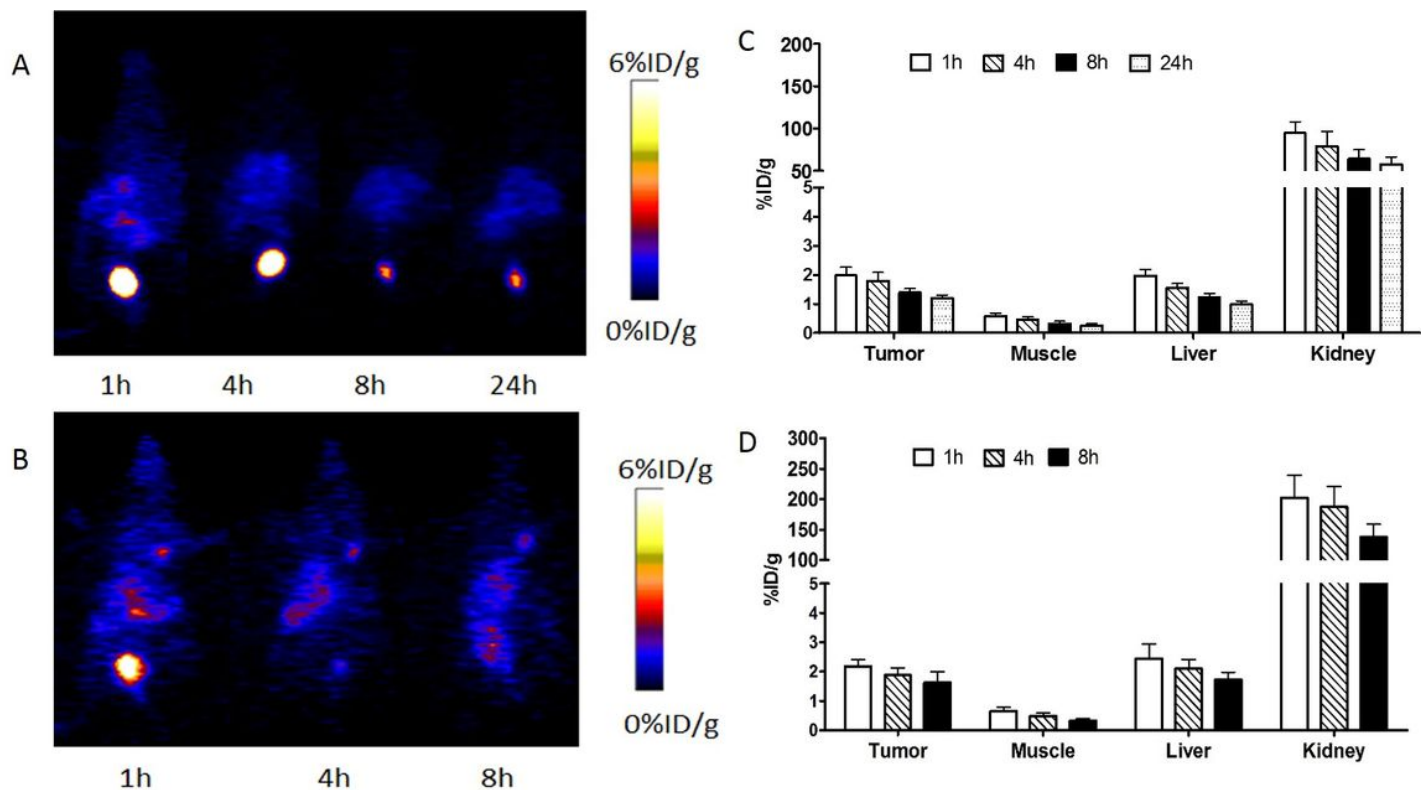


**Figure 7**

Decay-corrected whole-body PET images of mice bearing MCF-7 xenografts (A) after injection of  $^{89}\text{Zr}$ -DFO-MAL-Cys-MZHER2 ; B) PET images of mice bearing SKOV-3 xenografts after injection of the tracer under block. C) Quantification of  $^{89}\text{Zr}$ -DFO-MAL-Cys-MZHER2 in MCF-7 xenografts models and SKOV-3 xenografts models in the presence of excess block agents (D) respectively.

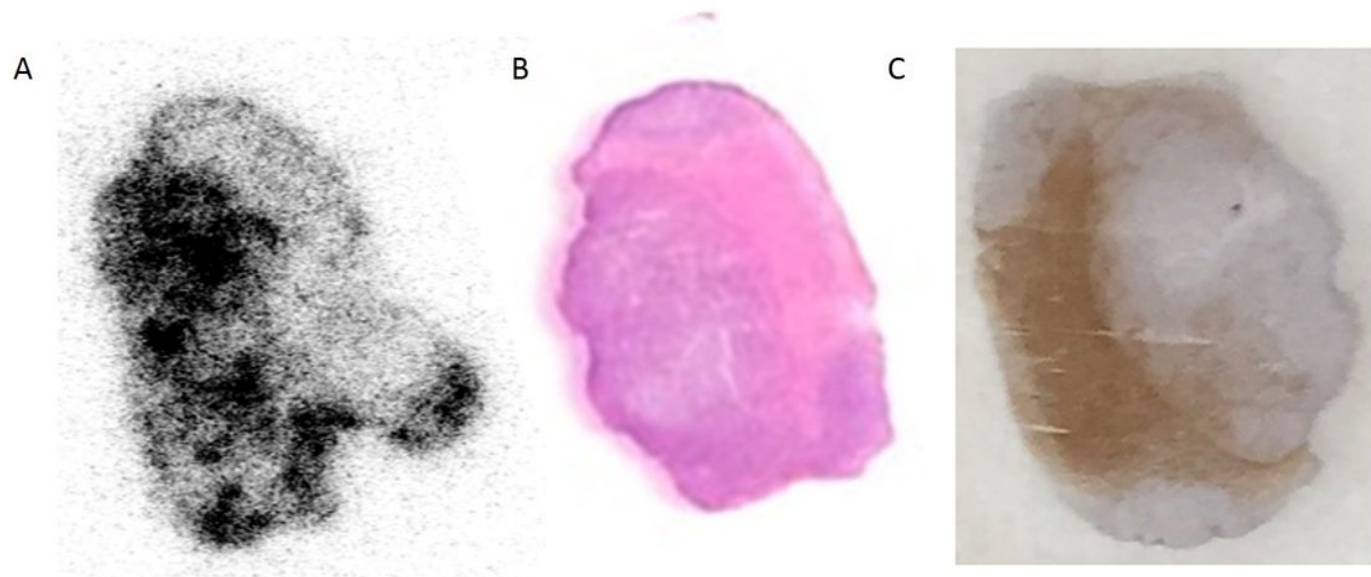


**Figure 8**

A) Autoradiographic distribution of  $^{89}\text{Zr}$ -DFO-MAL-Cys-MZHER2 in tumor slices. HE staining (B) and immunohistochemical image (C) of HER2 in tumor slices.

## Supplementary Files

This is a list of supplementary files associated with this preprint. Click to download.

- [Table1.docx](#)